

## Thermal Non-Destructive Testing with Effective Biomaterial for Bone Density Diagnosis: A Numerical Study

Sanchita Dass<sup>1</sup>, Juned A Siddiqui<sup>1a</sup>

<sup>1,2</sup> Department of Electronics, Medi-Caps University Indore, (M.P.), India

<sup>a</sup>Email: [juned.siddiqui@medicaps.ac.in](mailto:juned.siddiqui@medicaps.ac.in)

### Abstract

Nanoscale biomaterials play an active role in the medical field. These materials are used for different applications, such as biological system repair, replacement, stimulation, and interaction. This encourages us to seek out bio-materials that can be helpful to enhance the detection capabilities of active thermography. This non-destructive testing technique (NDT) yields such promising results that it can be used as a screening tool for the early detection of bone diseases. Hence, in this work, we used modulated active thermography with iron oxide nanoscale biomaterial to detect bone density. Normally, modulated active thermography uses a post-processing scheme to improve depth penetration; hence, this work utilized a pulse compression-based technique. This study focuses on the effect of biomaterial coating on bone with varying densities when using active thermography. We are using a three-dimensional FEM bone model with different density variations for this. We also compare the coated and non-coated resolutions using the signal-to-noise ratio (SNR). Furthermore, we discovered that the iron oxide coating can improve the current thermal NDT technique.

**Keywords:** *NDT; SNR, Biomaterial, Bone density*

### 1. Introduction

Active infrared thermography (IRT) is a non-destructive technique for diagnosing that uses external heat simulation and records surface temperature variation. Because of its safe, non-contact, non-invasive, and wide-area inspection characteristics, it has gained critical importance in the field of non-destructive testing and evaluation for biomedical applications in recent years. This thermal wave imaging, which has a wide range of applications in the diagnosis of various diseases based on thermal contrast analysis, can also be used to determine variations in bone density. A controlled stimulus is applied to the subject, and the resulting response is recorded. To diagnose density variation, additional processing techniques are used to study the thermal map over skin [3]. The most commonly used active TNDT approaches, depending on the object to be inspected and the external stimulus, are pulse thermography (PT), lock-in thermography (LT), and pulse phase thermography (PPT) [5]. However, these conventional methods of pulse and pulse phase

necessitate high peak power [6], and lock-in necessitates repetitive injection of mono-frequency sinusoidal heat flux to locate defects at different depths. To overcome the limitations of traditional thermal wave imaging techniques (depth resolution peak power), linear-frequency modulated thermal wave imaging [7] (LFMTWI) is proposed, which can be performed with moderate peak power heat sources in a shorter time span than conventional pulse and lock-in based thermographic methods [8]. This study shows how to use the FMTWI technique for bone diagnostics [11], specifically by considering the bone with tissue, skin, and muscle over layers. To test the efficacy of the proposed method, LFMTW is applied to a modelled bone sample along with a bio-material coating [9]. A bone sample with different stages of osteoporosis and a bio-material coating is modelled using finite element analysis and simulated with a frequency modulated stimulus in this paper [10]. Further, pulse compression and Fourier analysis techniques are used as post-processing schemes for better detection, and their performance with signal-to-noise ratios is compared with coated and non-coated bone models.

## 2. Heat simulation and postprocessing

As shown in fig 1, we used LFMWI heat stimuli with frequencies ranging from 0.01 to 0.5 Hz and lasting 100 seconds. In this technique, modulated thermal waves with a suitable frequency band and equal energies are probed into the test sample to detect defects at various depths. It can be expressed as

$$f(t) = A e^{j2\pi(f_1 + Rt)t} \quad (1)$$

'A' is the flux amplitude, 'f1' is the modulated frequency, R is the sweep rate, and 't' is the time.

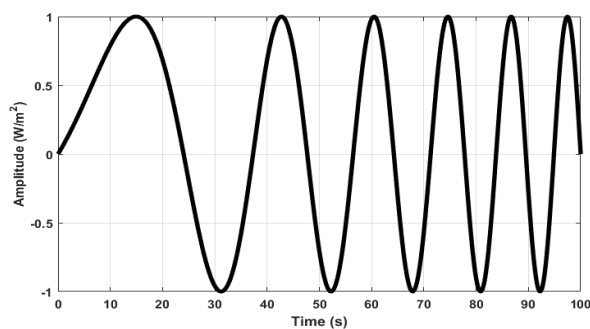


Fig. 1. Schematic of Linear Frequency Modulated Signal imposed on bone sample.

In this paper, we use a post processing technique based on pulse compression. Each pixel temperature profile is assumed to be a time sequence in the IRT. These patterns include a temporal thermal response and an active response that correspond to the offset in excitation. Cross correlation is performed between the temperature time sequence distribution of the selected reference pixel and the time delayed version of the pixel over the sample to obtain an active response. The difference in temporal temperature responses provides information about defective and non-defective regions that are dependent on the thermal properties of the material. This captured temperature time sequence distribution can be recaptured using the following formula:

$$\text{Correlation - Coefficient}(CC) = \text{IFFT} \{RT(\omega) * OT(\omega)\} \quad (2)$$

Here, The Fourier transforms of the chosen reference response and temporal temperature response at a given location are denoted by  $RT(\omega)$  and  $OT(\omega)$ .

## 3. Experimentation and Simulation

A 3D Finite Element Analysis (FEA) of a human bone sample was performed to test the proposed model. The modelled bone sample is made up of

different layers with varying thicknesses, including skin (0.5 mm), fat (0.5 mm), muscle (0.5 mm), and bone (2.5 mm). In order to visualise the different stages of osteoporosis, the bone region was further comprised of four artificial abnormalities, each with a diameter of 20 mm and different thermal properties such as Density, Thermal Conductivity, and Specific Heat. Table 1 shows the sample thermal properties of the holes on bone region.

Table 1. Thermal Properties [27]

Region	Density ( $\rho$ ) (Kg m <sup>-3</sup> )	Thermal Conductivity (k) (W m <sup>-1</sup> K <sup>-1</sup> )	Specific Heat (c) (J Kg <sup>-1</sup> K <sup>-1</sup> )
Skin	1109	0.37	3391
Fat	911	0.21	2348
Muscle	1090	0.49	3421
Bone	2420	0.616	1430
D1	1480	0.25	1200
D2	1200	0.34	2000
D3	2090	0.532	1235
D4	2310	0.588	1365

Table 2. Iron oxide thermal Properties [28]

Nanoparticles	Density ( $\rho$ ) (Kg m <sup>-3</sup> )	Thermal Conductivity (k) (W m <sup>-1</sup> K <sup>-1</sup> )	Specific Heat (c) (J Kg <sup>-1</sup> K <sup>-1</sup> )
Iron oxide	5240	0.3	103.9

The front end (skin surface) of modelled sample is excited by imposing a Linear Frequency Modulation with a 500 W m<sup>-2</sup> heat flux during active heating, the corresponding temporal temperature response over the skin surface was recorded at a frame rate of 33 frames per second. The simulations were run under non-isothermal boundary conditions, with the sample at 310.15 K normal body temperature. The simulated data recorded over the skin is then analysed in the frequency domain. As shown in Fig 2, FEA is performed on a modelled specimen coated with a thermo-active biomaterial. Furthermore, AWGN with an SNR of 60 dB is artificially inserted into the simulated data so that the proposed method can be used in real-time situations.

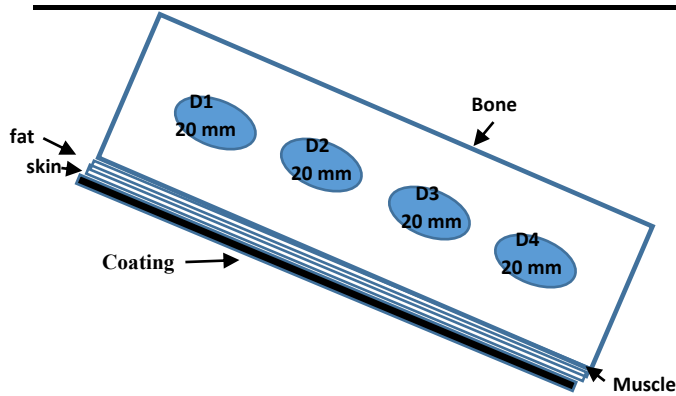


Fig. 2. Layout of the bone sample with biomaterial coating.

#### 4. Results and discussion

This study demonstrates the efficacy of the bio-material (Iron-oxide) in conjunction with the linear frequency modulated thermal wave imaging technique. The results show that the contrast achieved in Correlation – Coefficient (CC) image with the bio-material coating on the bone is superior to that achieved in conventional Correlation – Coefficient (CC) image without any coating. This could be because the Iron oxide nano-particles have improved thermal properties. Fig 3 and 4 depicts the measured SNR values for circular shaped bone defects with and without biomaterial coating. The results show that images with biomaterial coating have higher SNR values than images without coating.

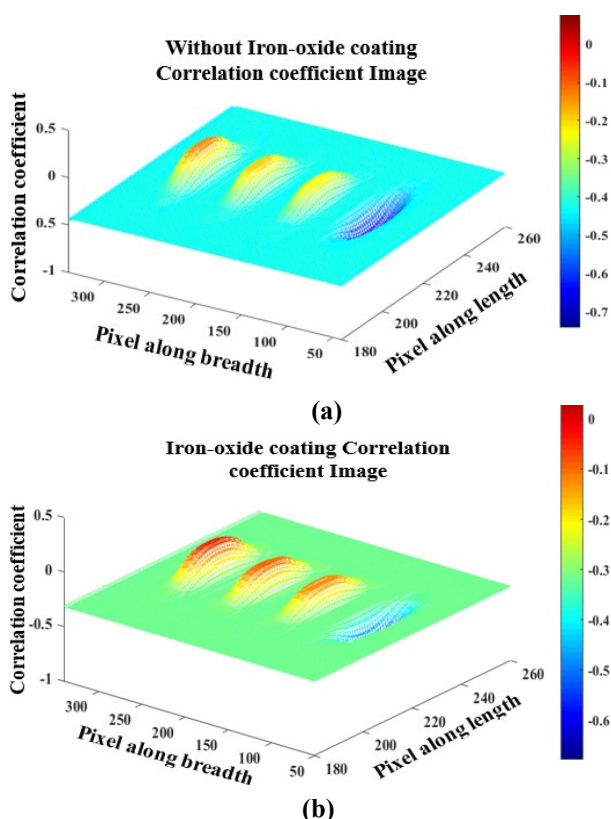


Fig. 3. Simulation results of (a) non-coated and (b) coated bone sample

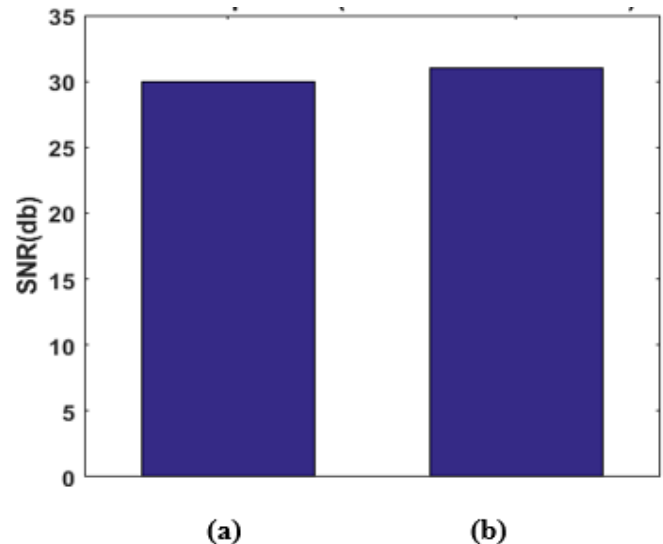


Fig. 4. SNR Comparison (a) non-coated and (b) coated bone sample

#### 5. Conclusions

The frequency modulated thermal wave imaging technique is used in this paper to detect bone density variation with a Iron oxide nanoparticle coated sample using a finite element modelling approach. The proposed schemes' bone density detection capabilities are further quantified by taking SNR into account. The results clearly show that the bio-material Correlation images have a much higher contrast of visibility of defects when compared to the same images without bio-material LFM.

#### 6. References

- [1]. L. S. Nair and C. T. Laurencin, "Polymers as biomaterials for tissue engineering and controlled drug delivery," *Adv. Biochem. Eng. Biotechnol.*, vol. 102, pp. 47- 90, 2006, doi:10.1007/b137240.
- [2]. L. L. Hench, "Biomaterials: A forecast for the future," *Biomaterials*, vol. 19, no. 16, pp. 1419-1423, 1998, doi:10.1016/s0142-9612(98)00133-1.
- [3]. E. J. Nassar et al., \* *Biomaterials and Sol-Gel Process: A Methodology for the Preparation of Functional Materials*.
- [4]. C. M. Agrawal, "Reconstructing the human body using biomaterials," *JOM*, vol. 50, no. 1, pp. 31-35, 1998, doi:10.1007/s11837-998-0064-5.
- [5]. J. D. Bronzino, *The Biomedical Engineering Handbook*, 2nd ed, vol. 2, 2000.
- [6]. A. B. H. Yoruc and B. C. Sener, "Biomaterials" in Prof. Kara S, editor. *A roadmap of biomedical engineers and*

- milestones, ISBN: 978-953-51-0609-8, 2012.
- [7]. D. Campoccia et al., "A review of the biomaterials technologies for infection-resistant surfaces," *Biomaterials*, vol. 34, no. 34, pp. 8533-8554, 2013, doi:10.1016/j.biomaterials.2013.07.089.
- [8]. K. Chaloupka et al., "Nanosilver as a new generation of nanoparticle in biomedical applications," *Trends Biotechnol.*, vol. 28, no. 11, pp. 580-588, 2010, doi:10.1016/j.tibtech.2010.07.006.
- [9]. A. A. Adedoyin and A. K. Ekenseair, "Biomedical applications of magnetoresponsive scaffolds," *Nano Res.*, vol. 11, no. 10, pp. 5049-5064, 2018, doi:10.1007/s12274-018-2198-2.
- [10]. X. P. V. Maldague, *Theory and Practice of Infrared Technology for Non Destructive Testing*. New York: Wiley, 2001.
- [11]. H. I. Ringermacher et al., "Flashquenching for high resolution thermal depth imaging," *Proc. AIP*, vol. 700, pp.477-481, 2004.
- [12]. F. B. D. Djupkep et al., "Analysis of a new method of measurement and visualization of indoor conditions by infrared thermography," *Rev. Sci. Instrum.*, vol. 84, no. 8, p. 084906, 2013, doi:10.1063/1.4818919.
- [13]. S. Nayak et al., "Systematic review and metaanalysis of the performance of clinical risk assessment & instruments for screening for osteoporosis or low bone density," *Osteoporos. Int.*, vol. 26, no. 5, pp. 1543-1554, 2015, doi:10.1007/s00198-015-3025-1.
- [14]. G. Dua and R. Mulaveesala, "Infrared thermography for detection and evaluation of bone density variations by non-stationary thermal wave imaging," *Biomed. Phys. Eng. Express*, vol. 3, no. 1, p. 017006, 2017, doi:10.1088/2057-1976/aa5b4d.
- [15]. A. Sharma et al., "Linear frequency modulated thermal wave imaging for estimation of osteoporosis: An analytical approach," *Electron. Lett.*, vol. 56, no. 19, pp. 1007-1010, 2020, doi:10.1049/el.2020.0671.
- [16]. L. Feng et al., "Lock-in thermography and its application in nondestructive evaluation," *Infrared Laser Eng.*, vol. 39, pp. 1121-1123, 2010.
- [17]. D. P. Almond and S. G. Pickering, "An analytical study of the pulsed thermography defect detection limit," *J. Appl. Phys.*, vol. 1, p. 093510, 2012.
- [18]. A. Levy et al., "A new thermography-based approach to early detection of cancer utilizing magnetic nanoparticles theory simulation and in vitro validation," *Nanomedicine*, vol. 6, no. 6, pp. 786-796, 2010, doi:10.1016/j.nano.2010.06.007.
- [19]. Y. Ohashi and I. Uchida, "Applying dynamic thermography in the diagnosis of breast cancer," *IEEE Eng. Med. Biol. Mag.*, vol. 19, no. 3, pp. 42-51, 2000, doi:10.1109/51.844379.
- [20]. P. Raverkar, J. A. Siddiqui, A. Kulkarni and R. Mulaveesala, "Corrosion detection in mild steel using effective post processing technique for modulated thermal imaging: A numerical study," 2021 IEEE International Conference on Technology, Research, and Innovation for Betterment of Society (TRIBES), 2021, pp. 1-4, doi: 10.1109/TRIBES52498.2021.9751651.
- [21]. R. Mulaveesala and V. S. Ghali, "Cross-correlation based approach for thermal nondestructive characterization of carbon fiber reinforced plastics," *Insight*, vol. 53, no. 1, pp. 34-36, 2011, doi:10.1784/insi.2011.53.1.34.
- [22]. V. S. Ghali et al., "Three dimensional pulse compression for infrared nondestructive testing," *IEEE Sens. J.*, vol. 9, no. 7, pp. 832-833, 2009, doi:10.1109/JSEN.2009.2024042.
- [23]. J. A. Siddiqui et al., "Modelling of the frequency modulated thermal wave imaging process through the finite element method for non-destructive testing of a mild steel sample *Insight, Non-Destruct. Test. Cond. Monit.*, vol. 57, pp. 266-268, 2015.
- [24]. R. Mulaveesala et al., "Pulse compression approach to infrared nondestructive characterization," *Rev. Sci. Instrum.*, vol. 79, no. 9, p. 094901, 2008, doi:10.1063/1.2976673.
- [25]. G. Dua et al., "Effect of spectral shaping on defect detection in frequency modulated thermal wave imaging," *J. Opt.*, vol. 17, no. 2, pp. 1-5, 2015, doi:10.1088/2040-8978/17/2/025604.
- [26]. A. Sharma et al., "Novel analytical approach for estimation of thermal diffusivity and

- effusivity for detection of osteoporosis,” *IEEE Sens. J.*, vol. 20, no. 11, 6046-6054, 2020, doi:10.1109/JSEN.2020.2973233.
- [27]. S. R. H. Davidson, Heat transfer in bone during drilling Master of Applied [Science thesis] University of Toronto, 1999.
- [28]. L. Zhang et al., “Enhanced thermal conductivity for nanofluids containing silver nanowires with different shapes,” *J. Nanomater.*, vol. 2017, 1-6, 2017, doi:10.1155/2017/5802016.
- [29]. R. Mulaveesala and S. Tuli, “Theory of frequency modulated thermal wave imaging for non-destructive subsurface defect detection,” *Appl. Phys. Lett.*, vol. 89, no. 19, p. 191913, 2006, doi:10.1063/1.2382738.
- [30]. V. Arora and R. Mulaveesala, “Pulse compression with Gaussian weighted chirp modulated excitation for infrared thermal wave imaging,” *Prog. Electromagn. Res. Lett.*, vol. 44, pp. 133-137, 2014, doi:10.2528/PIERL13111301